Autorotation Path Planning Using Backwards Reachable Set and Optimal Control

Shane Tierney and Jack W. Langelaan
Aerospace Engineering, Penn State University

This paper presents a methodology to compute the backwards reachable set from safe on ground to a trimmed autorotation condition. This backwards reachable set represents the region of the trimmed autorotation state space from which safe paths to touchdown at a specified point are guaranteed to exist. The backwards reachable set is found by computing optimal trajectories from candidate initial states (distance and height above the touchdown point, horizontal speed, descent rate, rotor speed) to the designated touchdown point. In addition, the set of trimmed autorotation conditions which are likely to lead to safe trajectories to ground are computed. As an example, the safe landing set is computed for a generic utility helicopter.

Nomenclature

C	Cost Function
c_{d0}	Main Rotor Profile Drag Coefficient
C_P	Power Coefficient
C_T	Thrust Coefficient
C_x	Horizontal Component of Thrust coefficient
C_z	Vertical Component of Thrust coefficient
x	Horizontal distance from touchdown point
f_e	Fuselage Equivalant Flat Plate Area
f_g	Ground Effect Factor
f_I	Induced Velocity factor
h	Height above touchdown point
H_R	Rotor Height
I_R	Main Rotor Polar Moment of Inertia
m	mass
R	Main Rotor Diameter
u	horizontal velocity
v	Induced Velocity
v_h	Hover Induced Velocity
w	descent rate
α	Main Rotor Tip Path Plane Angle
λ	Main Rotor Inflow Ratio
σ	Main Rotor solidity Ratio
ρ	Air Density
Ω	Main Rotor Angular Speed
θ	Aircraft Pitch Angle

Introduction

There is considerable interest in the use of autonomous helicopters for tasks such as resupply and casualty evacuation. Further, sensor packages carried by some autonomous rotorcraft (such as the FORESTER radar carried by the A160 Hummingbird) are becoming very complex (and hence expensive). Loss of a payload (or worse, a loss of patient undergoing transport to a medical facility) is thus becoming a critical concern, and safe recovery in the event of vehicle failure is a critical technology. Power loss, in particular, is a vehicle failure which is known to be recoverable through autorotation landing.

However, autorotation is an extremely difficult maneuver. Safety of autorotation continues to be a significant concern to the manned rotorcraft community. The final phase (i.e. flare) of the maneuver is especially difficult, requiring precise control and timing for success, while the consequences of failure include severe damage to the vehicle and injury or death to the pilot or passenger. Practice autorotation thus continues to be a part of the training curriculum for military pilots, but this is a dangerous aspect of training, since a significant number of accidents occur during practice. This is mitigated somewhat in multi-engine aircraft, however unmanned rotorcraft are typically single-engine vehicles.

A critical problem is the flare to touchdown. Computing a safe, feasible flare trajectory in real time is extremely difficult because of the high dimensionality of the problem, the limited computational resources likely to be available, and the likelihood of external disturbances such as gusts. Moreover, if an incorrect steady descent state is chosen there may not be a safe, feasible flare trajectory to landing.

A significant amount of research has been conducted on optimal path planning for both powered flight (Ref. 1) and autorotation (Refs. 2–4). In addition, the use of optimal control for autorotation flight training pilot cueing has been reported (Refs. 5, 6). More recently Abbeel et al. have demonstrated a machine-learning based approach to autorotation landings (Ref. 7) and a model-predictive control ap-

Presented at the 2010 AHS Forum.
Corresponding author: Jack Langelaan
(jlangelaan@psu.edu)

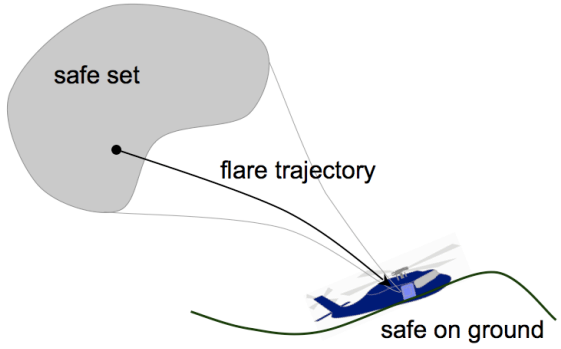

Fig. 1. Schematic of the guaranteed safe set: the set of trimmed autorotation states and initial points that are guaranteed to have a safe, feasible path to landing.

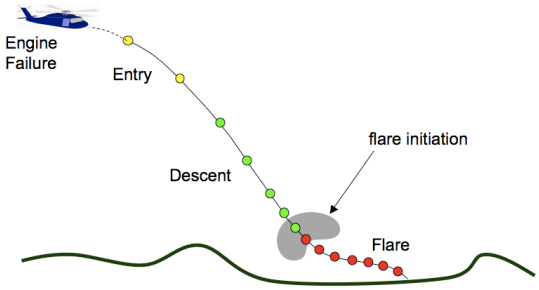

Fig. 2. Autorotation scenario.

proach is described by Dalamagkidis (Ref. 8).

In (Ref. 5) Aponso et al. note three important points: first, vehicle parameters such as weight can have a strong influence on the computed trajectory; second, a critical improvement would be the ability to continuously update trajectories to account for performance differences as well as errors in trajectory following; third, optimal trajectory planning can be used to expand the V-h envelope. Further, the previous work on autorotation does not account for disturbances (e.g. gusts, or even steady wind fields) or the effect on non-uniform terrain on autorotation, flare and landing. Thus there is still a need for significant research before the problem of autonomous autorotation can be completely solved.

The work presented in this paper focuses on finding the region of the vehicle's state space from which a safe, feasible path to landing is guaranteed to exist. This region of the state space is denoted the *safe landing set* and includes flare initiation point (as distance from and height above the touchdown point), forward speed, descent rate and rotor speed (see Figure 1). Here the state space is restricted to the set of trimmed autorotation conditions. An additional focus is the *probably safe landing set*, that part of the set of trimmed autorotation conditions which are likely to end in safe landing. This is distinct from the safe landing set because the flare initiation point is not specified.

The safe landing set is thus the backwards reachable set from safe-on-ground: any vehicle which enters the safe landing set is guaranteed to have a safe, feasible path to landing. The use of backwards reachable sets for safe (powered) landing of fixed wing aircraft has been reported (Refs. 9, 10), but the authors are unaware of backwards reachable set computations for rotorcraft landing (powered or unpowered).

This paper discusses the safe landing set and develops a methodology for computing the safe landing set (and the associated probably safe set). This is applied to a model of a utility helicopter and some of the implications are discussed. Since optimal control is used to find the safe landing set some aspects of the optimal flare trajectories are also described.

Problem Definition

The problem consists of finding safe, feasible paths from engine failure to touchdown. Given a desired landing site, the nominal flight path from engine failure to landing is assumed to consist of three phases: first, engine failure and entry to a stable steady-state autorotation condition; second, steady descent in this autorotation condition, finally flare and landing (see Figure 2).

The purpose of this paper is to develop a methodology to enable computation of the set of all steady state autorotation conditions which are likely to result in a safe flare to landing. Safe and feasible, in this case, mean that all controls and states stay within predefined allowable limits throughout the flight and touchdown occurs with descent rate, forward speed, position, and pitch angle within acceptable limits. Ultimately this safe landing set will include the effects of external disturbances such as wind; in this paper only the deterministic case is considered.

Given the vehicle state

$$\mathrm{x} = \begin{bmatrix} x_{ip} & z_{ip} & u & w & \Omega \end{bmatrix}^T \tag{1}$$

where the subscript ip denotes flare initiation point and $[u\ w\ \Omega]^T$ are taken from the set of all trimmed autorotation conditions

$$\mathscr{A} = \left\{ \mathrm{a}_i | \mathrm{a}_i = [u\ w\ \Omega]^T \right\} \tag{2}$$

the safe landing set is defined as

$$\mathscr{S} = \left\{ \mathrm{s}_i | \mathrm{s}_i = [x_{ip}\ z_{ip}\ u\ w\ \Omega]^T,\ [u\ w\ \Omega]^T \in \mathscr{A} \right\} \tag{3}$$

Here $\mathrm{s}_i \in \mathscr{S}$ means that a safe, feasible trajectory to touchdown exists from s_i. Thus any trajectory that guides the helicopter from the moment of engine failure in to $\mathscr{S}$ is guaranteed to end in a safe landing at a particular desired touchdown point. The safe set is shown schematically in Figure 1.

A further set, denoted the probably safe landing set, consists of those autorotation trim conditions a_i which are likely to end in a safe landing. This is denoted as

$$\tilde{\mathscr{A}} = \{\tilde{\mathrm{a}}_i\} \tag{4}$$

This set does not include particular choices of flare initiation position x_{ip} and z_{ip}, and thus it cannot guarantee safe landing: a member of $\tilde{\mathscr{A}}$ may have safe paths to landing from some flare initiation points but not others. The set $\tilde{\mathscr{A}}$ is the projection of $\mathscr{S}$ onto $\mathscr{A}$. Any trajectory that guides the helicopter from the moment of engine failure to a point in $\tilde{\mathscr{A}}$ is likely to result in a safe landing somewhere. Note that the touchdown point cannot be specified here: it will be dependent on the particular flare initiation point.

Thus this paper has two aims: first, computing the safe landing set $\mathscr{S}$; second, computing the probably safe landing set $\tilde{\mathscr{A}}$. The key point is finding members of $\tilde{\mathscr{A}}$ which have safe paths to landing from as large a region of the space $[x_{ip}\ z_{ip}]^T$ as possible.

The safe landing set thus has two purposes: first, it provides a target region for guidance of the mid-phase of autorotation descent; second, it defines conditions where flare should be initiated to allow touchdown at a specified location. The probably safe set defines the autorotation trim conditions which are most likely to result in safe landing, and thus provides information to the mid-phase descent trajectory.

Computing the Safe Landing Set

The safe landing set is found by repeatedly solving a trajectory optimization problem from an initial state to a specified touchdown point. The trajectory optimization problem is cast as a non-linear parameter optimization problem by discretizing system dynamics and finding the control inputs which minimize a cost function (discussed later).

Vehicle Dynamics

Equations of motion are derived by Aponso (Ref. 3) and repeated without derivation here:

$$\dot{x} = u \tag{5}$$

$$\dot{h} = -w \tag{6}$$

$$m\dot{u} = \rho(\pi R^2)(\Omega R)^2 C_x - \frac{1}{2}\rho f_e u\sqrt{u^2+w^2} \tag{7}$$

$$m\dot{w} = mg - \rho(\pi R^2)(\Omega R)^2 C_z - \frac{1}{2}\rho f_e w\sqrt{u^2+w^2} \tag{8}$$

$$I_R\Omega\dot{\Omega} = P_s - \frac{1}{\eta}\rho(\pi R^2)(\Omega R)^2 C_P \tag{9}$$

$$\dot{P}_s = \frac{1}{\tau_p}(P_{res} - P_s) \tag{10}$$

Because the work presented here focuses on the flare phase of the autorotation trajectory, it is assumed that the helicopter has been in autorotation long enough for residual engine power, P_{res}, to decay away. Equation 7 then simplifies to the identity $0 = 0$. Also, the helicopter pitch angle, θ, is assumed to be approximately equal to the tip path plane angle, α, and is replaced in kind.

Coefficients are defined as:

$$C_P = \frac{1}{8}\sigma c_{d_0} + C_T\lambda \tag{11}$$

$$C_x = C_T\sin(\alpha) \tag{12}$$

$$C_z = C_T\cos(\alpha) \tag{13}$$

$$\lambda = \frac{u\sin(\alpha) - w\cos(\alpha) + v}{\Omega R} \tag{14}$$

The induced velocity is:

$$v = K_{ind} v_h f_I f_G \tag{15}$$

where v_h is the reference (hover) induced velocity, f_I is the ratio of actual induced velocity to the reference v_h, and f_G accounts for the decrease in induced velocity due to ground effect:

$$v_h = (\Omega R)\sqrt{\frac{C_T}{2}} \tag{16}$$

$$f_I = \begin{cases} 1/\sqrt{b^2 + (a+f_I)^2} & if (2a+3)^2 + b^2 \geq 1 \\ a(.373a^2 + .598b^2 - 1.991) & otherwise \end{cases} \tag{17}$$

a and b are given as:

$$a = \frac{u\sin(\alpha) - w\cos(\alpha)}{v_h} \tag{18}$$

$$b = \frac{u\cos(\alpha) + w\sin(\alpha)}{v_h} \tag{19}$$

$$f_G = 1 - \frac{R^2\cos^2(\theta_W)}{16(h+H_R)} \tag{20}$$

$$\cos^2(\theta_w) = \frac{(-wC_T + vC_z)^2}{(-wC_T + vC_z)^2 + (uC_T + vC_x)^2} \tag{21}$$

As an additional simplification, ground effect was ignored (i.e. $f_G = 1$). This should increase the conservativeness of the solutions since it ignores the improvement in rotor performance at low altitude (Ref. 11).

Written in compact form, dynamics in autorotation are

$$\dot{\mathrm{x}} = f(\mathrm{x}, \mathrm{u}) \tag{22}$$

where the inputs are $\mathrm{u} = [C_T\ \alpha]^T$. Trim states can be found by setting $\dot{\mathrm{x}} = 0$ and solving for x given a feasible u.

The problem of computing flare trajectories now consists of finding the input sequence $\mathrm{u}(t)$ which results in a

safe landing. One approach is to discretize the problem, assuming that the input is constant over some interval. This will result in a parameter optimization problem. Typically the problem is discretized in time: for the case considered here the time required to fly a path depends on the inputs, and time becomes an additional parameter in the optimization problem. It is therefore more convenient to discretize the problem in height (since the final altitude of the helicopter is specified as $h_f = 0$). In this case inputs are assumed to be constant over an interval Δh (see Figure 3).

This discretization is performed by first integrating the dynamics one step forward in time using a forward Euler integration, so that

$$\mathrm{x}_{k+1} = \mathrm{x}_k + \dot{\mathrm{x}}_k \Delta t_k \tag{23}$$

and then computing Δt_k in terms of the altitude interval Δh_k and the descent rate $\dot{h}_k$ over that interval:

$$h_{k+1} = h_k + \dot{h}_k \Delta t_k = h_k + \Delta h_k \tag{24}$$

Hence

$$\Delta t_k = \frac{\Delta h_k}{\dot{h}_k} \tag{25}$$

The system dynamics can now be written as

$$\mathrm{x}_{k+1} = \mathrm{x}_k + \dot{x}\frac{\Delta h_k}{\dot{h}_k} \tag{26}$$

$$= \mathrm{x}_k + \left(\frac{\dot{\mathrm{x}}_k}{\dot{h}_k}\right)\Delta h_k \tag{27}$$

Hence

$$\mathrm{x}_{k+1} = \mathrm{x}_k + \left.\frac{d\mathrm{x}}{dh}\right|_k \Delta h_k \tag{28}$$

Recognizing that $\dot{h}_k = -w_k$ (from vehicle kinematics) and using Aponso's equations of motion, the components of $\left.\frac{d\mathrm{x}}{dh}\right|_k$ are

$$\frac{dx}{dh} = -\frac{u}{w} \tag{29}$$

$$\frac{dt}{dh} = -\frac{1}{w} \tag{30}$$

$$\frac{du}{dh} = -\frac{1}{mw}(\rho(\pi R^2)(\Omega R)^2 C_x - \frac{1}{2}\rho f_e u\sqrt{u^2+w^2}) \tag{31}$$

$$\frac{dw}{dh} = -\frac{1}{mw}(mg - \rho(\pi R^2)(\Omega R)^2 C_z - \frac{1}{2}\rho f_e w\sqrt{u^2+w^2}) \tag{32}$$

$$\frac{d\Omega}{dh} = -\frac{1}{I_R \Omega w}(P_s - \frac{1}{\eta}\rho(\pi R^2)(\Omega R)^2 C_P) \tag{33}$$

The time-index subscript has been dropped for clarity. Note that height is no longer a part of the state vector: it is now an independent variable. Time has taken its place. It will be assumed that the helicopter is always descending, so $\dot{h} < 0$ and $\Delta h_k < 0$. Thus

$$\Delta t = \frac{dt}{dh}\Delta h > 0 \tag{34}$$

This approach contains two implicit assumptions: first, the helicopter is always descending during final approach (i.e. no "swoops"); second, the time interval Δt_k is short enough that changes in descent rate can be ignored.

The state vector has now become

$$\mathrm{x} = \begin{bmatrix} x & t & u & w & \Omega \end{bmatrix}^T \tag{35}$$

Safe, Feasible Flare Trajectories

The trajectory planning problem is now a parameter optimization problem:

$$\text{minimize } C(\mathrm{x}_{0\ldots K}, \mathrm{u}_{0\ldots K-1}) \tag{36}$$

$$\text{subject to } \mathrm{x}_{k+1} = \mathrm{x} + \left.\frac{d\mathrm{x}}{dh}\right|_k \Delta h_k \tag{37}$$

$$\mathrm{x}_{min} \le \mathrm{x}_k \le \mathrm{x}_{max} \tag{38}$$

$$g(\mathrm{x}_k) \le 0 \tag{39}$$

$$\mathrm{u}_{min} \le \mathrm{u}_k \le \mathrm{u}_{max} \tag{40}$$

where $g(\mathrm{x}_k)$ represents state-dependent constraints such as structural load limits and the set of free parameters is the input sequence $\mathrm{u}_{0\ldots K-1}$.

In the autorotation flare problem the cost is a function of distance from the desired landing condition, i.e.

$$C_{td} = (\mathrm{x}_K - \mathrm{x}_{des})^T \mathrm{W}_{td} (\mathrm{x}_K - \mathrm{x}_{des}) \tag{41}$$

where x_{des} is the desired touchdown condition and W_{td} is a weight matrix.

The problem is expressed as an interior-point problem by defining state constraints as an additional cost:

$$C_{state} = \sum_{k=1}^{K} c(\mathrm{x}_k) \tag{42}$$

Here c is a barrier function of the form

$$c(x) = \frac{1}{(x - x_{min})^2} + \frac{1}{(x_{max} - x)^2} \tag{43}$$

The final cost function is

$$C(\mathrm{x}_{0\ldots K}, \mathrm{u}_{0\ldots K-1}) = C_{td} + \gamma C_{state} \tag{44}$$

where γ is a parameter that can be varied to change the relative weight of violating state constraints versus the touchdown cost.

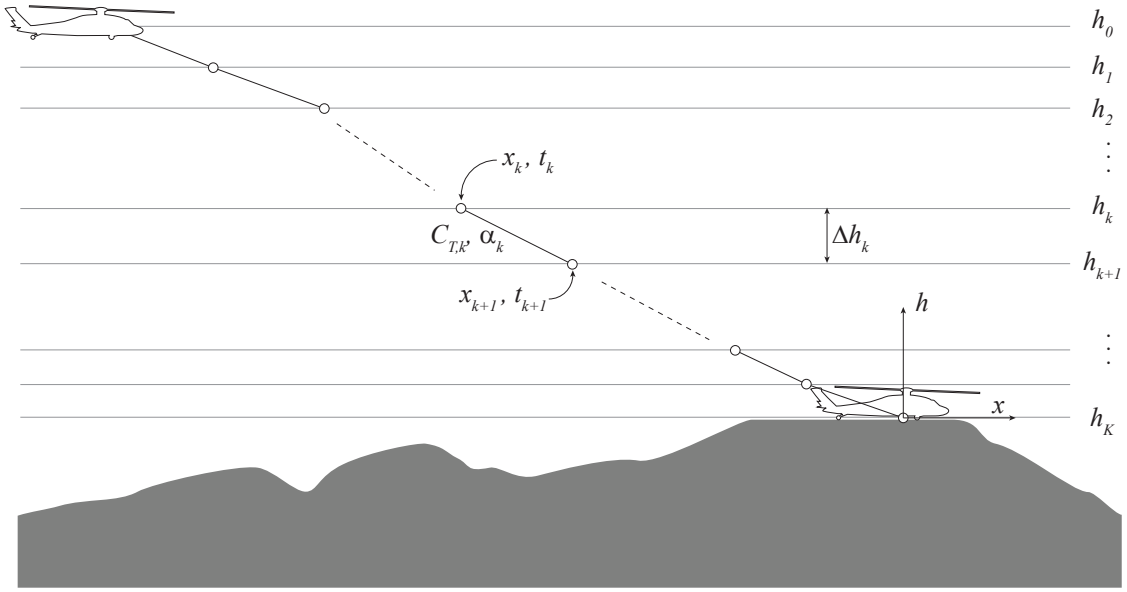

Fig. 3. Schematic of the discretized flare trajectory optimization problem. The target touchdown point is at the origin, the shaded region denotes terrain.

A gradient descent approach is used to iteratively solve this optimization problem for a particular initial state. The first iteration uses a large value of γ to ensure that a path which does not violate state constraints is found. If a path is found then γ is reduced and the optimization is run again using the previous solution as the initial guess. This is repeated until a path which is both feasible and safe (meaning that touchdown constraints are satisfied) is found. Thus the question of the existence of a feasible path has been expressed as an optimization problem: if the optimal path is not feasible, then a feasible path does not exist.

Solution Methodology

The guaranteed safe landing set is found by repeatedly solving the trajectory optimization problem defined in Equations 36 through 40 for candidate initial states

$$\hat{\mathrm{s}}_i = \left[x_{ip}\ z_{ip}\ \mathrm{a}_i^T\right]^T,\ \mathrm{a}_i \in \mathscr{A} \tag{45}$$

Figure 4 shows the trim set $\mathscr{A}$ for a generic utility helicopter with parameters given in Table 1.

To find $\mathscr{S}$, a candidate state $\hat{\mathrm{s}}$ is selected and the feasibility of a safe trajectory to touchdown is computed. If a safe, feasible trajectory exists then $\hat{\mathrm{s}} \in \mathscr{S}$. The procedure is summarized in Algorithm 1.

The Safe Landing Set for a Utility Helicopter

The safe landing set $\mathscr{S}$ and the maximum likelihood safe landing set $\tilde{\mathscr{A}}$ are computed for a generic utility helicopter

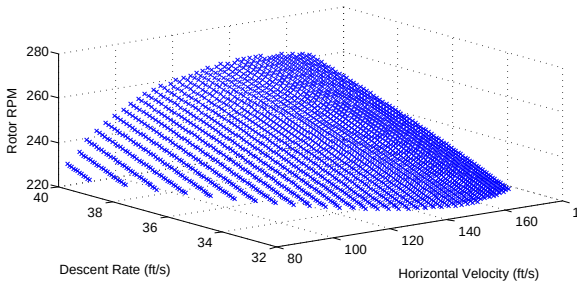

Fig. 4. Autorotation trim states for a generic utility helicopter.

with parameters given in Table 1 and state and control limits given in Table 2. Note that many of the limits are quite conservative, leading to overly conservative computation of the safe landing set. Here the terrain slope is assumed to be flat.

A set of evenly spaced flare initiation points ranging from 75 feet to 1500 feet horizontally and 25 feet to 700 feet vertically from the desired touchdown point was defined. To limit computation time a subset of evenly spaced autorotation trim conditions was chosen from the set of all autorotation trim conditions, and these were combined to define the set of candidate states.

For this problem the touchdown limits are given in Table 3. The touchdown cost weight matrix is

$$\mathrm{W}_{td} = \mathrm{diag}\,(4,\ 0,\ 3,\ 4,\ 0) \tag{46}$$

The weight of zero on time reflects the lack of importance of a particular time of flight and the weight of zero on

Table 1. Parameters for generic utility helicopter

parameter	symbol	value
blade cord	c	1.75 feet
rotor profile drag coefficient	C_{d0}	0.02
equivalent flat plate area	f_e	27.58 feet^2
rotor height	H_r	9.417 feet
main rotor polar oment of inertia	I_R	1512.6 feet^4
induced power factor	K_{ind}	1.05
number of blades	N_B	4
rotor diameter	R	26.83 feet
gross weight	W	16638 lbs
power efficiency factor	η	0.97
air density	ρ	2.134×10^{-3} slugs/foot^3

Algorithm 1 Compute safe landing set.

1: $\mathscr{S} = \emptyset$, $\tilde{\mathscr{A}} = \emptyset$
2: Select candidate $\hat{\mathrm{s}}_i = \left[x_{ip}\ z_{ip}\ \mathrm{a}_i^T\right]^T$
3: Compute optimal trajectory from $\hat{\mathrm{s}}_i$ to goal
4: **if** trajectory is feasible and safe **then**
5: $\quad \mathscr{S} = [\mathscr{S}\ \hat{\mathrm{s}}_i]$
6: $\quad \mathscr{A} = [\mathscr{A}\ \hat{\mathrm{a}}_i]$
7: **else if** Trajectory is feasible but not safe **then**
8: $\quad$ reduce γ
9: $\quad$ go to 3
10: **else if** Trajectory is safe but not feasible **then**
11: $\quad$ increase γ
12: $\quad$ go to 3
13: **else**
14: $\quad$ discard $\hat{\mathrm{s}}$
15: **end if**
16: **if** No more candidate states **then**
17: $\quad$ Return $\mathscr{S}$, $\tilde{\mathscr{A}}$
18: **else**
19: $\quad$ go to 2
20: **end if**

rotor speed at touchdown indicates that this is also unimportant.

Safe Landing Set

The safe landing set is a high dimensional space (5 dimensional), hence visualization is difficult. Several projections onto 2D planes are presented and discussed.

Table 2. State and control limits for generic utility helicopter

state/control	symbol	upper	lower
forward speed	u	169 ft/s	0 ft/s
descent rate	w	40 ft/s	0 ft/s
rotor speed	Ω	360 rpm	225 rpm
blade tip path angle	α	10°	-10°
thrust coefficient	C_T	$1.5C_w$	0

Table 3. Touchdown safe conditions. $\theta_{terrain}$ is the terrain slope at the touchdown point (0° here).

state	upper	lower
x position	+25 ft	-25ft
time	–	–
forward speed	+20 ft/s	-25 ft/s
descent rate	+15 ft/s	-4 ft/s
rotor speed	–	–
aircraft pitch angle	$\theta_{terrain} + 10^\circ$	$\theta_{terrain} - 10^\circ$

The set of safe flare initiation points is shown in Figure 5. Matching intuition, results show that higher altitude means that flare must be initiated farther from the touchdown point (otherwise the helicopter will overshoot).

The traditional means of determining safety of autorotation is the V-h diagram. The corresponding plot here is the projection of the safe landing set onto the V-h plane and at first glance this should be similar to the V-h diagram. However there are some critical differences. Recall that the safe landing set comprises trimmed autorotation conditions, while the V-h diagram is generated for powered straight and level flight. For the vehicle studied here trimmed autorotation is impossible at horizontal speeds below approximately 80 fps, limiting the lower bound of speeds. The projection of the safe landing set onto the V-h plane is shown in Figure 6. Initial points that are too high don't allow the helicopter to lose altitude fast enough, points that are too fast don't allow the helicopter to bleed off enough speed.

Figure 7 shows sample flight paths from three flare initiation points for slow, moderate and fast initial speeds, with the touchdown point at the origin.

A more detailed look at the control and state history of the paths shown in Figure 7 is given in Figure 8, Figure 9, and Figure 10. Tip-path-plane angle behaves as expected, tilting back and pushing up against the allowable limit for most of the flight time. Then at the end, the helicopter tilts forward to match the terrain angle, in these cases 0°.

Equation 46 indicates that the touchdown horizontal po-

sition and sink rate have the largest effect on touchdown cost, while forward speed has a smaller effect. Thus it would be expected that the helicopter would sacrifice slowing itsself horizontally in order to slow its descent rate at touchdown and to ensure that touchdown occurs near the origin. This is reflected in each of the three examples shown here. While sink rate and distance from the origin (visible in Figure 7) are both very near their goal locations, forward speed is close to its upper limit. Additionally, the forward speed remains high because the helicopter is tilted back as far as is allowable and has no more means to slow its forward speed.

The probably safe set

A desirable trim state is one that gives the largest number of available safe flare initiation points which still result in safe, feasible trajectories to landing, leaving room for small errors between predicted and actual flight path.

Figure 11 shows the number of safe initiation points found at each trim state normalized by the total number of safe initiation points. A high number means that a particular trim state is more likely to lead to safe landing, since there are many flare initiation points from which safe paths to ground result. This is a measure of the volume fraction of the region of flare initiation points which can result in safe landing for a particular trimmed autorotation condition. This plot shows that trim points with low horizontal velocity are more likely to result in safe paths to ground. From this plot, the trim state with the largest number of safe initial points is

$$\tilde{a} = [83.1\ 39.9\ 229.2]^T \tag{47}$$

Note that this will be sensitive to the spacing of flare initiation points: too wide a spacing will result in missing potential safe initiation points, skewing the results.

Figure 12 gives the safe flare initiation point set for the trim state with the most safe flare initiation points. Note the gap in safe initial points near $x = -1000$: this is likely due to the path optimizer failing to find a solution within the allowed number of iterations. Intuition suggests that these points should also be safe, since they are surrounded by safe initial points.

Uses and Limitations

In addition to defining safe autorotation conditions, the safe landing set can be used as a goal space for mid-phase trajectory planners. A particularly sophisticated mid-phase planner may choose to send the vehicle through the "thickest" portion of the safe landing set, thus providing maximum robustness for flare initiation and errors or disturbances in the final flare trajectory.

The probably safe set defines the autorotation trim conditions which are more likely to lead to safe landing. The choice an autorotation trim state for the mid-phase descent should include this as a consideration as part of the transition from the point of engine failure to the steady autorotation condition.

It is expected that the optimal paths used in computing the safe set can also be used for fast trajectory generation. As a helicopter in steady autorotation enters the safe landing set, a trajectory to the desired touchdown point can be selected based on the nearest points for which trajectories have been computed. A trajectory following algorithm can then guide the helicopter along this path.

The major limitation of the results presented here is the sparsity of points tested. Current work focuses on expanding the search space and increasing the point density of candidate safe states, with an emphasis on the boundaries of the safe set. Further, incorporating ground effect and expanding the allowable vehicle state envelope is likely to increase the size of the safe set.

Conclusions

A methodology for computing the set of points for which a safe, feasible autorotation trajectory to safe on ground is guaranteed to exist has been presented. This is the backwards reachable set from safe-on-ground to a trimmed autorotation condition.

The set is found using optimal trajectory planning from a candidate trimmed autorotation initial state to a specified touchdown location. In addition to the safe set (which includes a specified initial height and distance from touchdown), the probably safe landing set is defined as the set of trimmed autorotation conditions from which a safe path to landing at a specified touchdown point is likely to exist.

Results are presented for a limited number of initial states for a utility helicopter in steady state autorotation. These results show that there are clear regions of the autorotation trim space which are more likely to lead to a safe landing. In addition the state and control histories of some sample paths computed using the trajectory optimizer are discussed.

References

[1]Bottasso, C. L., Croce, A., Leonello, D., and Riviello, L., "Rotorcraft Trajectory Optimization with Realizability Considerations," *Journal of Aerospace Engineering*, Vol. 18, (3), July 2008, pp. 146–155.
doi: 10.1061/(ASCE)0893-1321(2005)18:3(146)

[2]Johnson, W., "Helicopter Optimal Descent and Landing after Power Loss," Technical Memorandum TM 73244, NASA Ames Research Center, Moffett Field, CA, May 1977.

[3]Aponso, B. L., Edward N. Bachelder, P., and Dongchan Lee, P., "Automated Autorotation for Unmanned Rotorcraft Recovery," AHS International Specialistsí Meeting on Unmanned Rotorcraft, Chandler, Arizona, USA, 2005.

[4]Lee, A. Y., Bryson Jr., A. E., and Hindson, W. S., "Optimal Landing of a Helicopter in Autorotation," *Journal of Guidance, Control, and Dynamics*, Vol. 11, (1), January-February 1988, pp. 7–12.

[5]Aponso, B., Lee, D., and Bachelder, E. N., "Evaluation of a Rotorcraft Autorotation Training Display on a Commercial Flight Training Device," Proceedings of the American Helicopter Society 61st Annual Forum, 2005.

[6]Bachelder, E. N. and Aponso, B. L., "Using Optimal Control for Helicopter Autorotation Training," Proceedings of the American Helicopter Society 59th Annual Forum, May 6-8 2003.

[7]Abbeel, P., Coates, A., Hunter, T., and Ng, A. Y., "Autonomous Autorotation of an RC Helicopter," International Symposium on Robotics, 2008.

[8]Dalamagkidis, K., Valavanis, K. P., and Piegl, L. A., "Autonomous Autorotation of an Unmanned Rotorcraft using Nonlinear Model Predictive Control," *Journal of Intelligent and Robotic Systems*, Vol. 57, (1-4), 2009, pp. 351–369.
doi: 10.1007/s10846-009-9366-2

[9]Sprinkle, J., Eklund, J. M., and Sastry, S. S., "Deciding to Land a UAV Safely in Real Time," Americna Controls Conference, Portland, OR, USA, 2005.

[10]Bayen, A. M., Mitchell, I. M., Oishi, M. M. K., and Tomlin, C. J., "Aircraft Autolander Safety analysis Through Optimal Control-Based Reach Set Computation," *Journal of Guidance and Control*, Vol. 30, (1), January-February 2007, pp. 68–77.
doi: 10.2514/1.21562

[11]Leishman, J. G., *Principles of Helicopter Aerodynamics*, Cambridge University Press, New York, NY, 2006, Chapter 5.

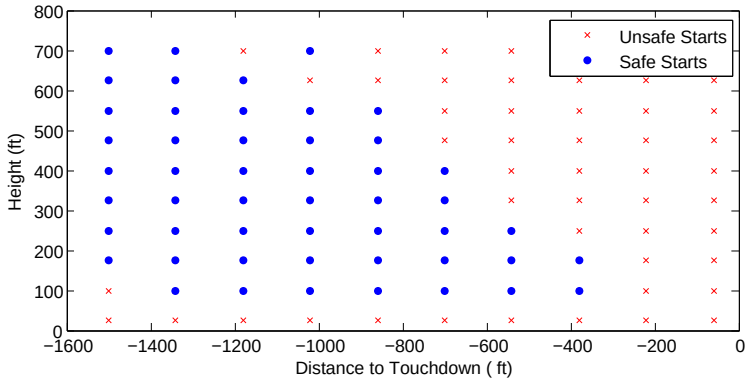

Fig. 5. Safe flare initiation locations for a generic utility helicopter

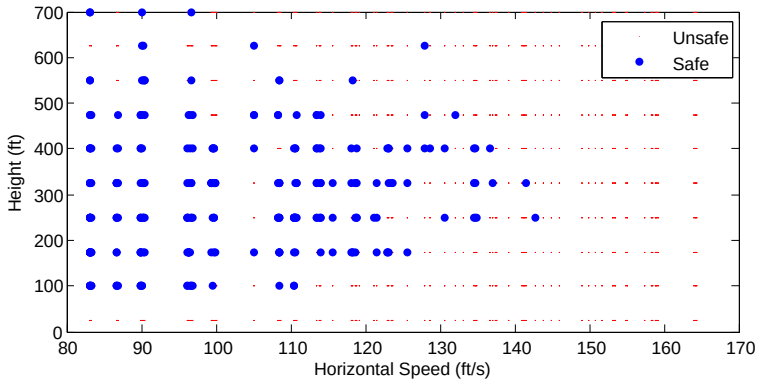

Fig. 6. Projection of the safe landing set onto the h-v plane.

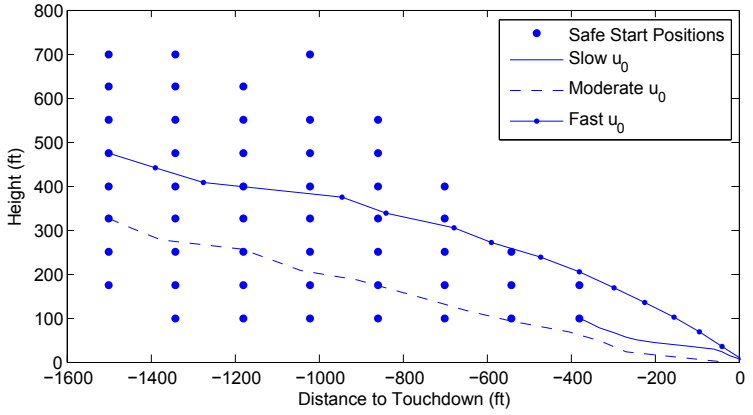

Fig. 7. Sample flare flight paths from three safe start locations

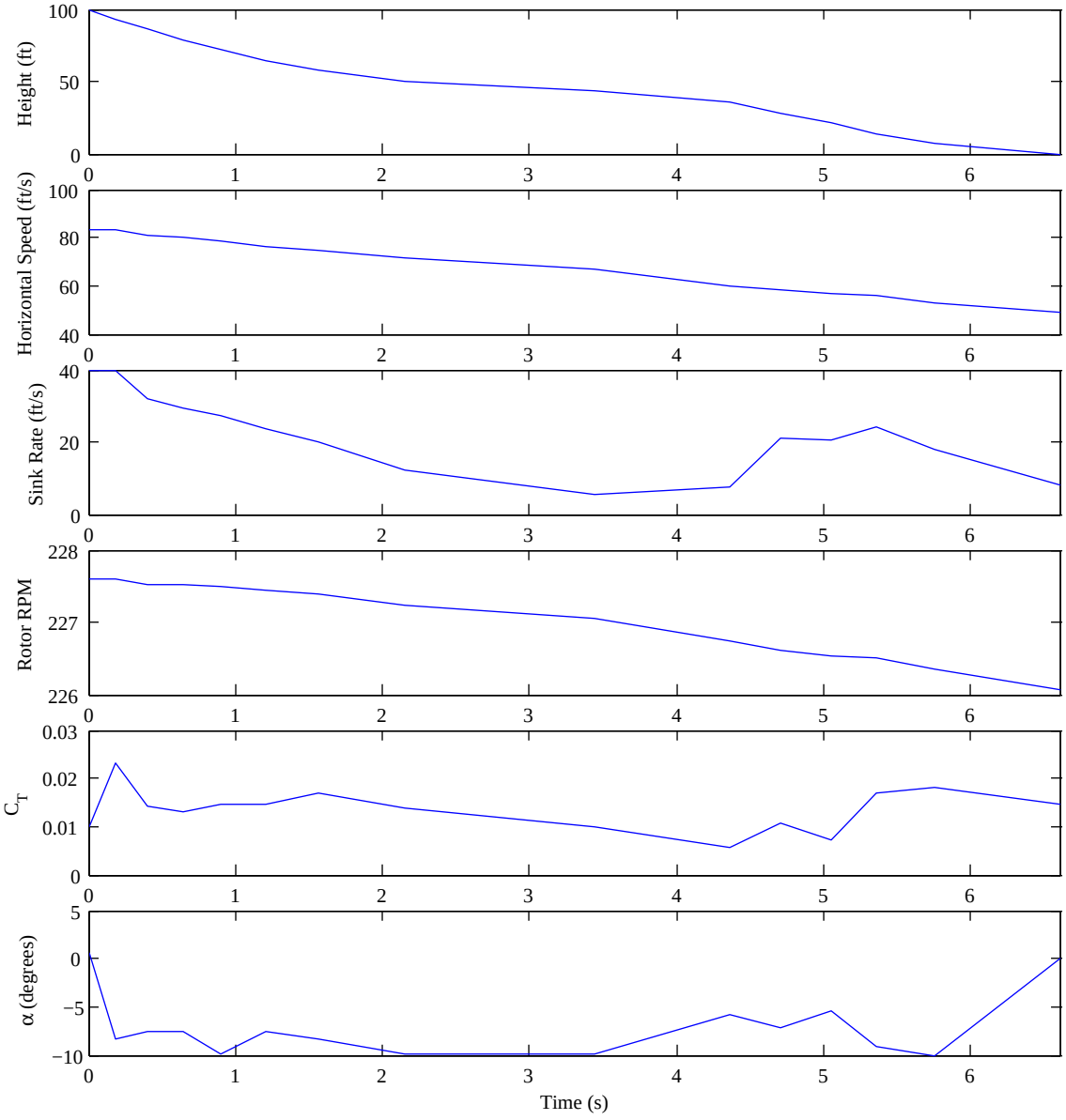

Fig. 8. State and control history for path denoted slow u_0 in Figure 7.

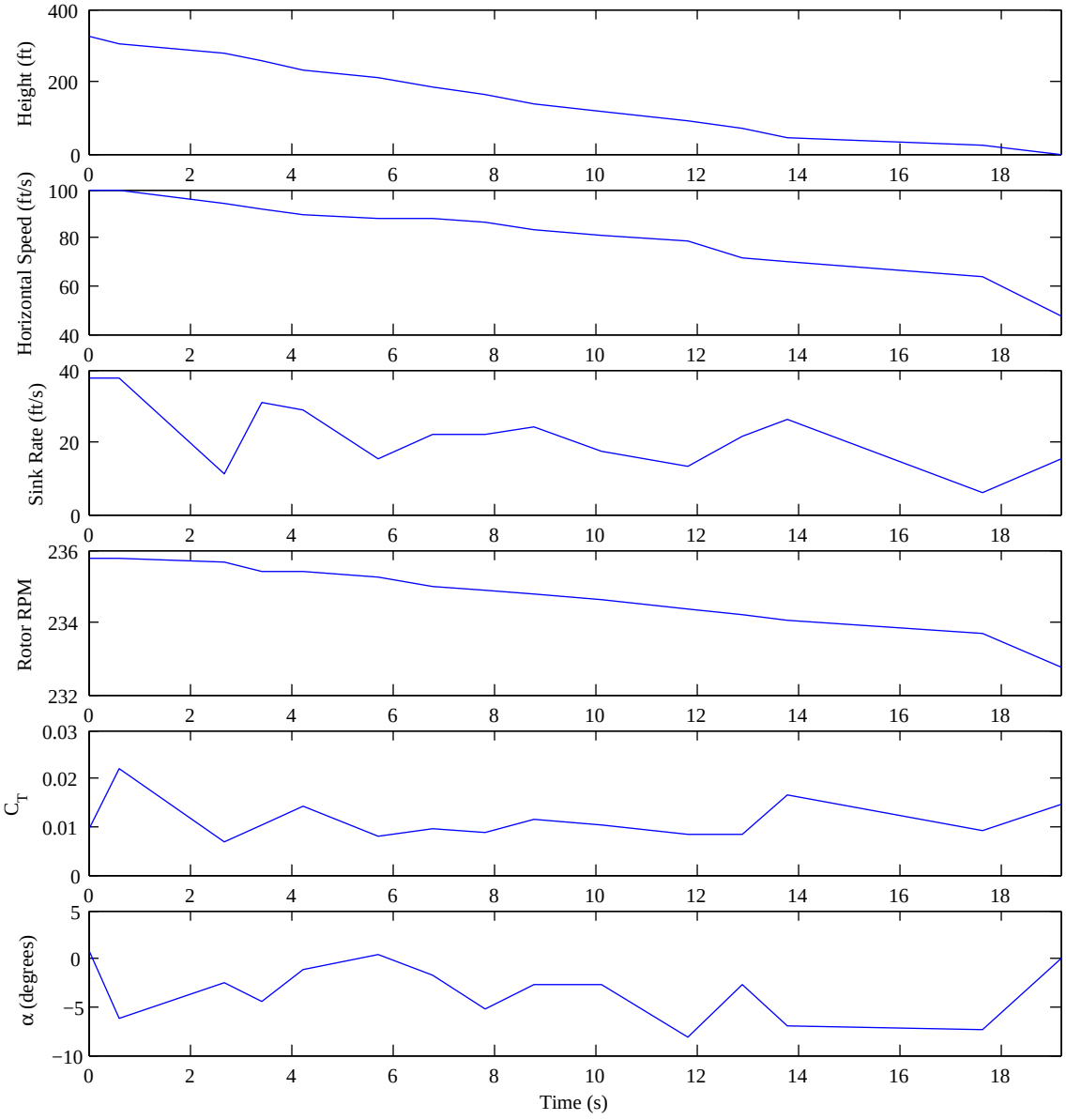

Fig. 9. State and control history for path denoted moderate u_0 in Figure 7.

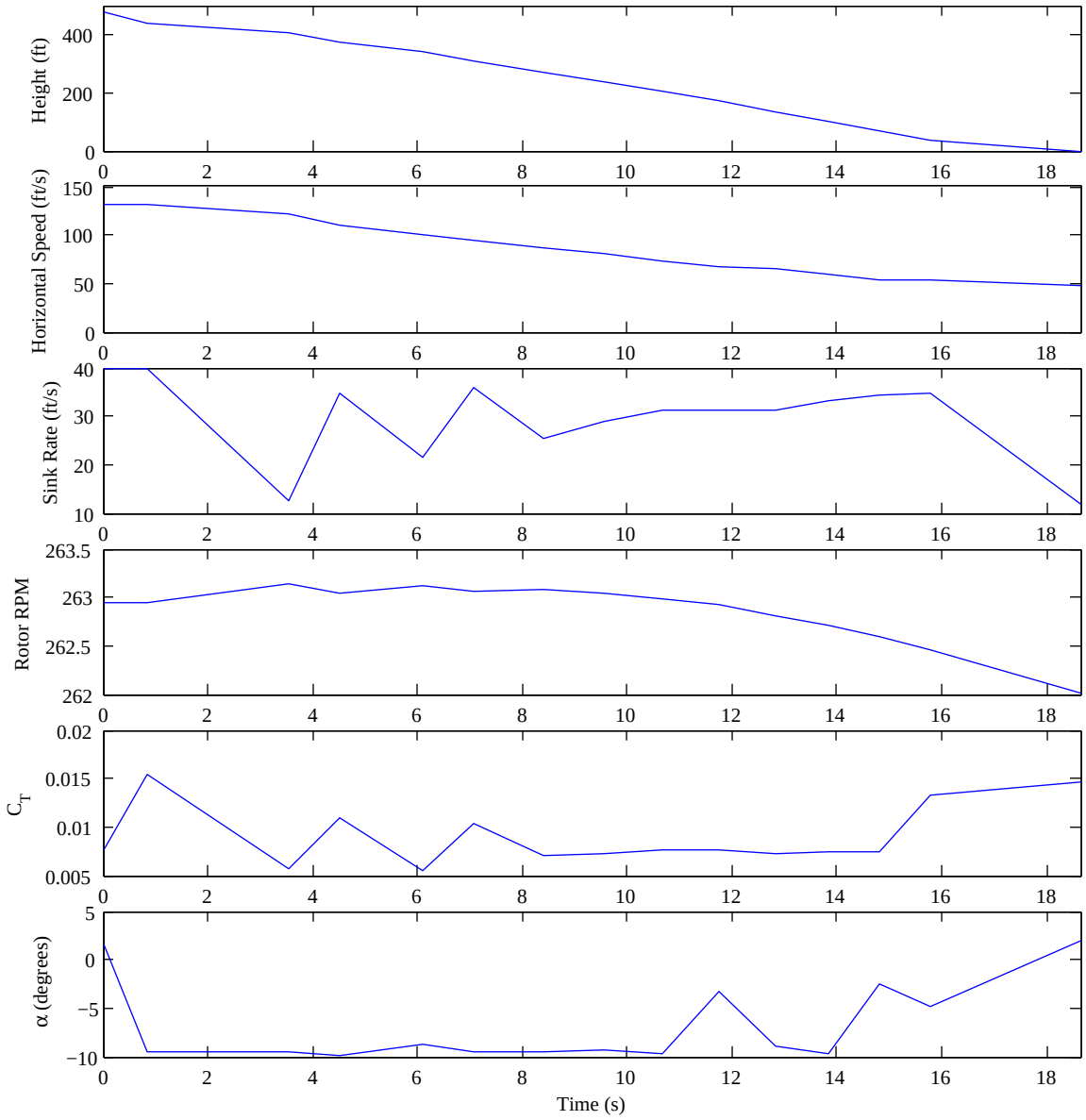

Fig. 10. State and control history for path denoted fast u_0 in Figure 7.

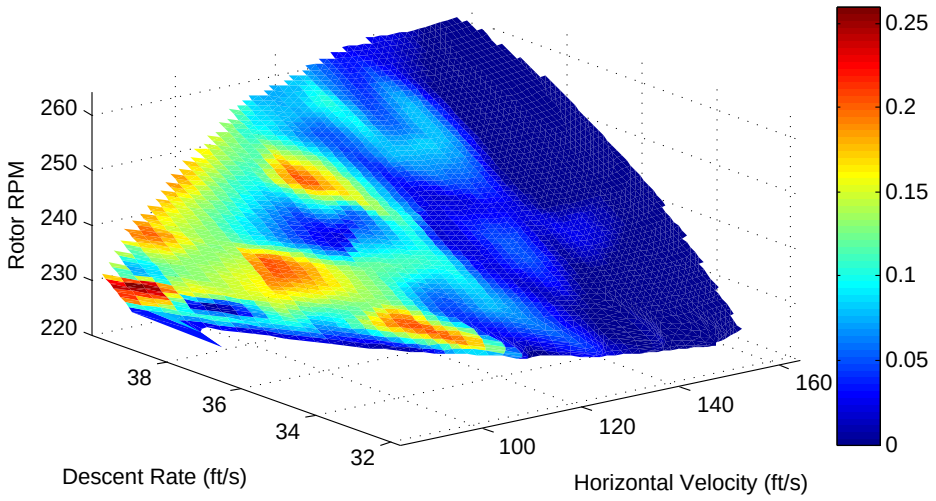

Fig. 11. Number of safe flare initiation positions reachable from each autorotation trim state. The "patchiness" in these results is in part due to choosing a fairly sparse set of initial trim conditions.

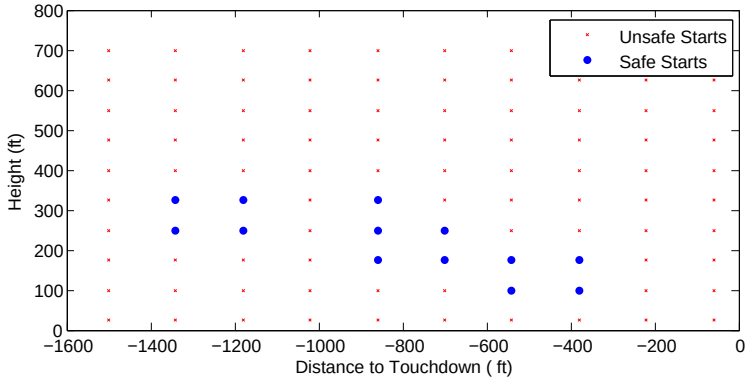

Fig. 12. Safe flare initiation points for the trim state with the higest number of safe initiation points.